Original Article
Regulatory mechanism of MiR-21 in formation and rupture of intracranial aneurysm through JNK signaling pathway-mediated inflammatory response

Zhihua Chen, Shuxin Song, Jianming Zhu, Xianliang Lai

Department of Neurosurgery, The Second Affiliated Hospital of Nanchang University, Nanchang, Jiangxi, China

Abstract: Objective: To investigate the regulatory mechanism of micro ribonucleic acid (miR)-21 in the formation and rupture of intracranial aneurysm through the c-Jun N-terminal kinase (JNK) signaling pathway-mediated inflammatory response. Methods: In the present study, the mice with miR-21 expression deficiency and over-expression in our laboratory were enrolled as the experimental group, while wild-type healthy mice were used as the control group. The mouse model of intracranial aneurysm was established by bilateral carotid artery ligation. The differences in the levels of key genes in the JNK signaling pathway (JNK1 and JNK2) were detected by fluorescence quantitative polymerase chain reaction (qPCR) and western blotting. At the same time, the changes in transcription and translation levels of inflammatory factors, interleukin-6 (IL-6), and tumor necrosis factor-α (TNF-α), in both groups were measured. After the mice were executed by an overdose of anesthesia, the morphology of the aneurysm in different objects was observed by Verhoeff-Van Gieson (EVG) staining and the expressions of TNF-α, JNK1, and JNK2 were determined by immunohistochemistry. Results: Compared with healthy mice, levels of JNK1 and JNK2 in mice with miR-21 deficiency were significantly decreased ($P < 0.05$) with a significant reduction of inflammatory factors IL-6 and TNF-α ($P < 0.05$). Compared with healthy mice, levels of JNK1 and JNK2 in mice with miR-21 over-expression were significantly increased ($P < 0.05$) with significant growing levels of inflammatory factors IL-6 and TNF-α ($P < 0.05$). The results of EVG staining revealed that the intracranial aneurysm was smaller in mice with miR-21 deficiency [(0.3 ± 0.12) cm] and larger in mice with miR-21 over-expression [(0.8 ± 0.25) cm] and there was a significant difference ($P < 0.05$). Moreover, the results of immunohistochemistry showed that the expression of TNF-α in intracranial aneurysm was obviously lower in mice with miR-21 deficiency than that in mice with miR-21 over-expression. Conclusion: MiR-21 can promote the production of inflammation-related factors through the JNK signaling pathway, leading to the formation and rupture of an intracranial aneurysm.

Keywords: miR-21, JNK signaling pathway, inflammatory response, intracranial aneurysm, inflammatory factors

Introduction

In recent years, great changes have taken place in the dietary habit. The unhealthy dietary habits, such as excessive intake of fat and insufficient exercise lead to cardiovascular and cerebrovascular diseases in different degrees [1]. According to statistics, for instance, the morbidity rate of cardiovascular and cerebrovascular diseases in China is approximately 2.5-3.2% [2]. Intracranial aneurysm has become one of the most lethal cerebrovascular diseases [3], increasing the psychological and economic burden on patients and their families due to its high morbidity and mortality rates. With the continuous development of molecular biological technique in recent years, the role of non-

coding ribonucleic acid (RNA) in the metabolic process *in vivo* has gradually attracted people's attention [4, 5]. For example, studies have found that the expression of micro RNA (miR)-21 is significantly higher at the pathogenic site in ovarian cancer and other tumors than that in normal tissues and organs [6]. The c-Jun N-terminal kinase (JNK) signaling pathway is one of the signaling pathways related to apoptosis and inflammatory response *in vivo* discovered in recent years. Studies have found that the JNK signaling pathway, an important component of the mitogen-activated protein kinase (MAPK) signaling pathway, mainly includes c-Jun N-terminal kinase, and participates in cytokine expression, proliferation, and apoptosis through phosphorylating the corresponding

Table 1. Fluorescence qPCR primers

Gene	Primer sequence
JNK1	F: 5'-AGTCACACCTGTCCTCTAG-3'
	R: 5'-ATCTGCCTATGCCTTGGTTG-3'
JNK2	F: 5'-GTGGCTGAGGAGATTCAAG-3'
	R: 5'-AAAGAAGGCATGAGAGCATC-3'
IL-6	F: 5'-AGCTAGCTACGATCCAGATCAG-3'
	R: 5'-CGAGCGATCAGCTACGATCG-3'
TNF-α	F: 5'-CGAGCGATCAGCTACGATC-3'
	R: 5'-CGAGCATCGATCGATCAGC-3'
GAPDH	F: 5'-TCATGGGTGTGAACCATGAGAA-3'
	R: 5'-GGCAGGACTGTGGTCATGAG-3'

proteins [7, 8]. In the present study, the regulatory mechanism of miR-21 in the formation and rupture of intracranial aneurysm through the JNK signaling pathway-mediated inflammatory response was explored for the first time. This provided a theoretical and experimental basis for the treatment of intracranial aneurysms.

Materials and methods

General data

In the present study, the mice with miR-21 deficiency and miR-21 over-expression constructed in our laboratory were taken as the experimental group, while the healthy mice were used as the control group. The mouse model of intracranial aneurysm was established by bilateral carotid artery ligation. Rats were used for all experiments and all procedures were approved by the Animal Ethics Committee of The Second Affiliated Hospital of Nanchang University.

Main reagents: The RPMI-1640 medium, high-glucose Dulbecco's modified Eagle medium (DMEM), and fetal bovine serum (FBS) were purchased from Roche (Indianapolis, IN, USA), 0.25% trypsin and EDTA from Invitrogen (Carlsbad, CA, USA), the lentiviral vector system and transfection kit from TAKARA, the RNA extraction kit from TAKARA (Dalian, Liaoning, China), the animal protein extraction kit, Verhoeff-Van Gieson (EVG) kit, enzyme-linked immunosorbent assay (ELISA) kit, and Matrigel medium used in cell invasion assay from Roche (Indianapolis, IN, USA).

Reverse transcription-polymerase chain reaction (RT-PCR)

RNA extraction: The RNA was extracted according to the instructions of the AXYGEN kit [9], as follows: (1) About 0.1 g cryo-preserved tissue samples were taken from liquid nitrogen, dissolved on ice, added with 0.45 mL RNA Plus, and ground into pieces in the pre-cooled mortar. Then, the samples were transferred into a 1.5 mL EP tube, added with 0.45 mL RNA Plus, washed, and transferred into a centrifuge tube. (2) 200 μL chloroform was added into the centrifuge tube, shaken violently for 15 s and placed on ice for 15 min, followed by (3) Centrifugation at 12000 rpm and 4°C for 15 min. (4) The supernatant was transferred into the RNase-free EP tube, added with an equal amount of isopropanol, mixed evenly and placed on ice for 10 min, followed by (5) Centrifugation at 12000 rpm and 4°C for 10 min. (6) The supernatant was discarded, and 750 μL 75% ethanol was added and mixed gently, followed by centrifugation at 12000 rpm and 4°C for 10 min. (7) The supernatant was discarded, and the residual ethanol was removed as far as possible. (8) An appropriate amount of RNase-free water was added and the mass of RNA extracted was determined, while the remaining RNA was use for reverse transcription [11].

Fluorescence quantitative PCR (qPCR)

In the present study, the fluorescence qPCR kit was purchased from TAKARA and the experiment was performed using the three-step method in accordance with the modified instructions. The primers used are shown in **Table 1**.

Western blotting

In the present study, the total protein was extracted from the samples using the animal protein extraction kit (Roche) according to the modified instructions [12]. Then the antibody was diluted at 1:5000 according to the instructions provided by Roche and western blotting was performed in accordance with the *Molecular Cloning Manual* [10].

Immunohistochemistry

Steps [11]: In the present study, the samples were detected using the immunohistochemical streptavidin-peroxidase (SP) method, as follows: (1) Different tissue samples were fixed with 10% formaldehyde, embedded in paraffin, and sliced into about 4 μm-thick sections. Then the sections were placed on the glass slide and baked at 60°C for about 2 h. (2) The sections were then deparaffinized with xylene, dehydrated with alcohol, treated with ultrapure water,

and washed with phosphate buffered saline (PBS) (pH 7.2) 5 times (5 min/time). Next, the sections were heated in a pressure cooker for about 2 min, cooled, and placed in PBS at room temperature for 30 min. (3) After PBS was removed, the sections were added with 50 µL peroxidase blocker, placed at 37°C for about 10 min, and washed with PBS 5 times (5 min/time). After PBS was removed, 45 µL nonimmune animal serum was added for incubation at room temperature for 10 min. (4) The sections were added with the primary antibody for incubation at room temperature for about 2 h or at 4°C overnight and washed with PBS 5 times (5 min/time). (5) 50 µL SP was added for incubation at room temperature for 2 h and the sections were washed with PBS 5 times (5 min/time). (6) After 100 µL developing solution was added, the sections were observed under a microscope. (7) After 10 min, the sections were rinsed with distilled water, counterstained with hematoxylin for 5 min, and rinsed again, followed by dehydration and drying with gradient alcohol and sealing with neutral balsam.

Identification of results

The yellow particles in the cell membrane or cytoplasm indicated the positive results of immunohistochemical staining. The immunohistochemical evaluation criteria are as follows [9]: membrane staining < 10% or negative tumor cells after staining: negative, only cell membrane staining or membrane staining > 10%: positive. The results were quantitatively determined using the KI index (the positive cell count in each field of view).

Determination of protein expression by ELISA [12]

ELISA was performed in accordance with the modified instructions of the ELISA kit (TAKARA) [12]. In the present study, the ELISA standard protein samples were diluted (1:50) using Assay Buffer and then the standard curve was plotted according to the instructions. The samples to be tested were diluted with PBS (pH 7.2) at 1:100, and then 100 µL samples were added into each well. Then 50 µL test solution was added into each well, and the TMB chromogenic substrate was also added after incubation at room temperature for 2 h. Finally, the absorbance was measured at 495 nm and the content and concentration of JNK1, JNK2, interleukin-6 (IL-6) and tumor necrosis factor-α (TNF-α) in each sample were calculated according to the standard curve.

EVG staining [13]

(1) The intracranial artery samples were taken from objects, baked at 58°C for 2 h, (2) deparaffinized, (3) soaked in Verhoeff's solution for 15 min until the tissue samples turned black, and (4) rinsed with tap water (direct washing should be avoided). (5) 2% ferric trichloride powder was added into different samples using the pipette for treatment for about 2 min. (6) Then the samples were treated with deionized water 3 times (3 min/time), and (7) treated with 1% sodium thiosulfate for 1 min. (8) Van Gieson was added for staining in a dark place for 10 min, and (9) the samples were dehydrated and (10) air dried.

Data processing

In this study, SPSS 20.0 software (SPSS Inc., Chicago, IL) was used for the statistical analysis of the experimental data obtained and the relevant measurement results were expressed as ($\bar{x} \pm s$). All experiments to date were derived from at least 3 independent experiments. The t test was used for the intergroup comparison and the chi-square test was used for enumeration data. Continuous data from multiple groups were analyzed by using one-way ANOVA, with the Tukey's post hoc test. *P*-values < 0.05 were considered statistically significant.

Results

Expression levels of blood miR-21, JNK1, JNK2, IL-6, and TNF-α in healthy mice and intracranial aneurysm mice were detected by fluorescence qPCR

To explore the correlation between miR-21 and inflammation-mediated intracranial aneurysm, the expression levels of miR-21, JNK1, JNK2, IL-6, and TNF-α in healthy mice and intracranial aneurysm mice were detected first. As shown in **Figure 1**, the level of miR-21 in intracranial aneurysm mice was significantly increased compared with that in healthy mice (*P* < 0.05). It was further found that the transcription levels of JNK1, JNK2, IL-6, and TNF-α in healthy mice were significantly lower than those in intracranial aneurysm mice (*P* < 0.05).

Expression levels of blood JNK1, JNK2, IL-6, and TNF-α proteins in healthy mice and intracranial aneurysm mice detected by ELISA

The expression levels of blood JNK1, JNK2, IL-6, and TNF-α proteins in healthy mice and
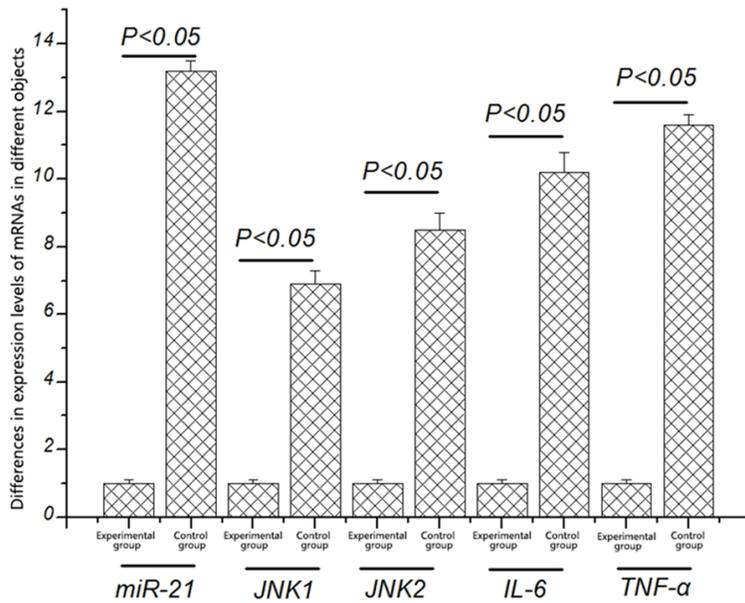
Figure 1. Differences in expression levels of miR-21, JNK1, JNK2, IL-6, and TNF-α in different objects. The expression levels of miR-21, JNK1, JNK2, IL-6, and TNF-α in experimental group are significantly higher than those in healthy mice ($P < 0.05$).
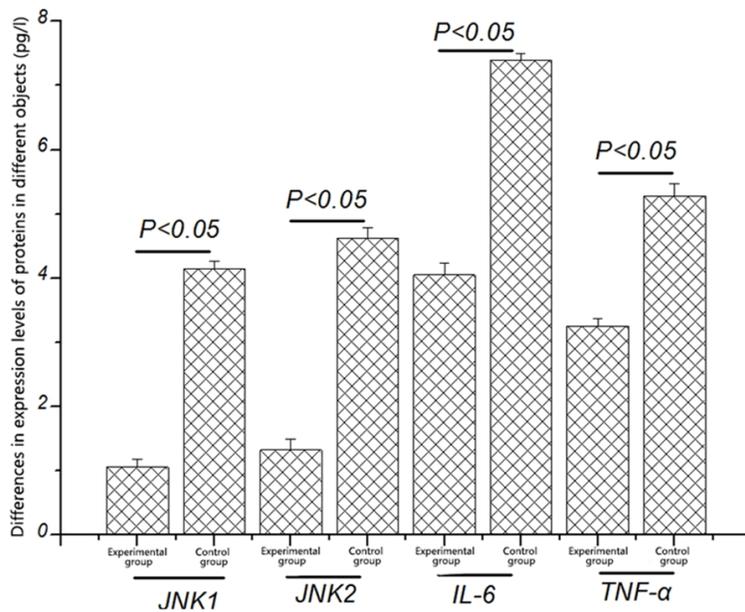
Figure 2. Differences in expression levels of JNK1, JNK2, IL-6, and TNF-α proteins in different groups. The expression levels of JNK1, JNK2, IL-6, and TNF-α proteins in experimental group are significantly higher than those in healthy mice ($P < 0.05$).

intracranial aneurysm mice were detected by ELISA. As shown in **Figure 2**, the levels of blood JNK1, JNK2, IL-6, and TNF-α proteins in intra-

cranial aneurysm mice were significantly increased compared with those in healthy mice [(4.15 ± 0.12) pg/L vs. (1.05 ± 0.12) pg/L, (4.62 ± 0.16) pg/L vs. (1.32 ± 0.17) pg/L, (7.39 ± 0.11) pg/L vs. (4.05 ± 0.18) pg/L, (5.28 ± 0.19) pg/L vs. (3.25 ± 0.11) pg/L] ($P < 0.05$), indicating that the up-regulation of transcription and protein expression of JNK1, JNK2, IL-6 and TNF-α is associated with intracranial aneurysm.

Transcription levels of JNK1, JNK2, IL-6, and TNF-α in mice with miR-21 deficiency and mice with miR-21 over-expression detected by fluorescence qPCR

It was found in the above experimental results that the expression of miR-21 in intracranial aneurysm mice was significantly higher than that in healthy mice, so it is speculated that miR-21 may be associated with the incidence of intracranial aneurysm. To explore the correlation between miR-21 and intracranial aneurysm, the transcription levels of JNK1, JNK2, IL-6, and TNF-α in mice with miR-21 deficiency and mice with miR-21 over-expression were detected. As shown in **Figure 3**, the transcription levels of JNK1, JNK2, IL-6, and TNF-α were obviously lower in mice with miR-21 deficiency than those in healthy mice ($P < 0.05$), while they were obviously higher in mice with miR-21 over-expression than those in healthy mice ($P < 0.05$). The above findings suggest that the reduction of miR-21 can inhibit the transcription levels of key genes in the JNK signaling pathway (JNK1 and JNK2) and inflammatory factors (IL-6 and TNF-α).
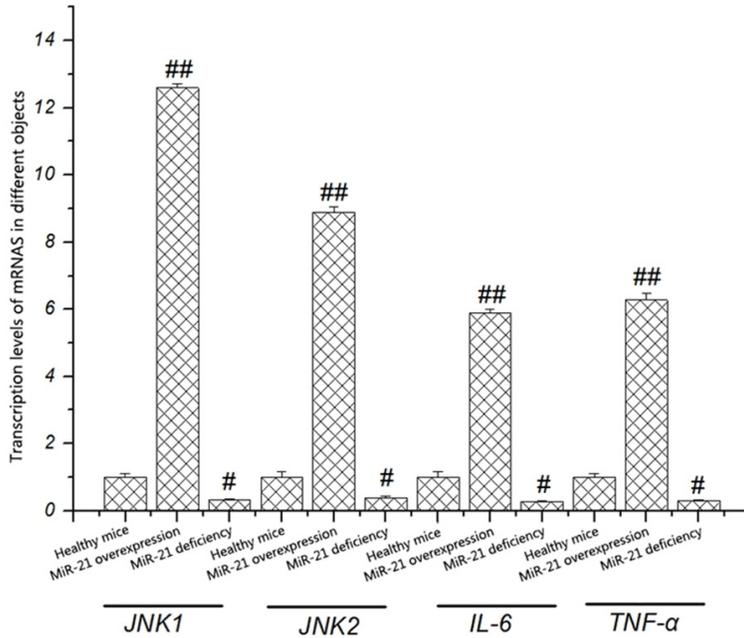
Figure 3. Transcription levels of JNK1, JNK2, IL-6, and TNF-α in different objects detected by fluorescence qPCR. The expression levels of JNK1, JNK2, IL-6, and TNF-α in mice with miR-21 over-expression are obviously higher than those in mice with miR-21 deficiency ($P < 0.05$).
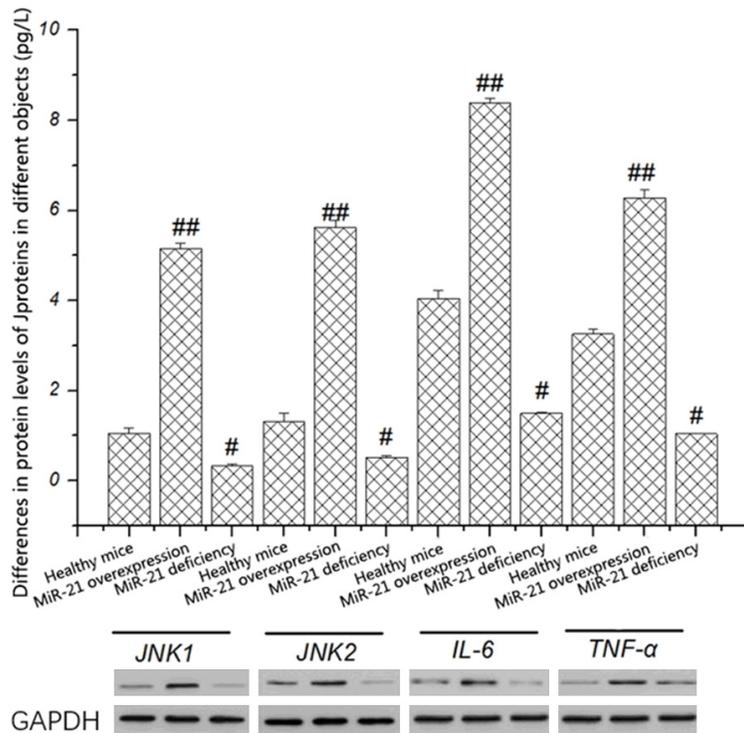
Figure 4. Differences in protein levels of JNK1, JNK2, IL-6, and TNF-α in different objects. The protein expression levels of JNK1, JNK2, IL-6, and TNF-α in mice with miR-21 over-expression are obviously higher than those in mice with miR-21 deficiency ($P < 0.05$).

Protein levels of JNK1, JNK2, IL-6, and TNF-α in mice with miR-21 deficiency and mice with miR-21 over-expression detected by western blotting

It was confirmed by fluorescence qPCR for the first time that the suppression of miR-21 can reduce the transcription levels of key genes in the JNK signaling pathway and inflammatory factors (IL-6 and TNF-α). To explore whether miR-21 affects the protein expression levels of the above genes, the protein levels of JNK1, JNK2, IL-6, and TNF-α in mice with miR-21 deficiency and mice with miR-21 over-expression were detected by western blotting. The results revealed that the protein levels of JNK1, JNK2, IL-6, and TNF-α were obviously lower in mice with miR-21 deficiency than those in healthy mice, while they were obviously higher in mice with miR-21 over-expression than those in healthy mice ($P < 0.05$) (**Figure 4**). The above results indicate that miR-21 can inhibit the expression of inflammatory factors through inhibiting the JNK signaling pathway, thereby reducing the occurrence of inflammatory response.

Expression levels of IL-6 and TNF-α in intracranial aneurysm mice detected by immunohistochemistry

The expression levels of IL-6 and TNF-α in mice with miR-21 deficiency and mice with miR-21 over-expression were detected by immunohistochemistry. The results showed that the expression levels of IL-6 and TNF-α at the lesion site in mice with miR-21 deficiency were remarkably lower than those in mice with miR-21 over-
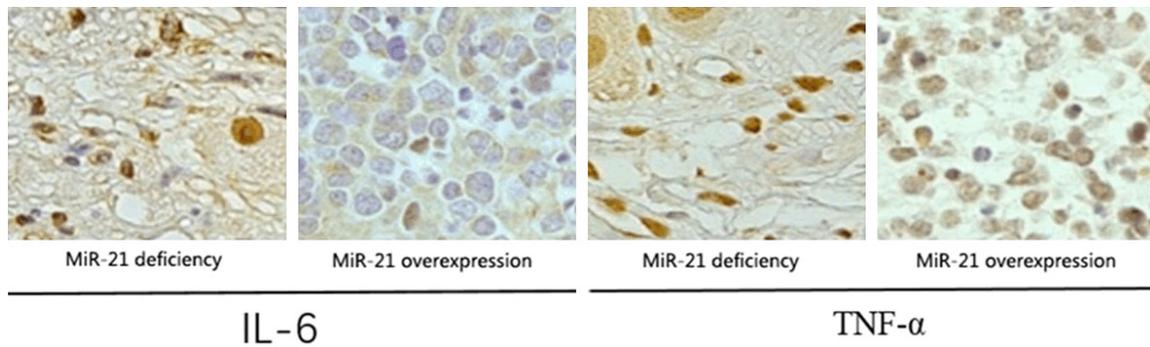
Figure 5. Expression levels of IL-6 and TNF-α in intracranial aneurysm mice detected by immunohistochemistry. The expression levels of IL-6 and TNF-α in mice with miR-21 deficiency are remarkably lower than those in mice with miR-21 over-expression ($P < 0.05$).

Figure 6. Size of intracranial aneurysm in different objects observed by EVG staining. In mice with miR-21 deficiency, the degrees of formation and rupture of intracranial aneurysm and the cranial arterial vascular thickness are significantly lower than those in mice with miR-21 over-expression ($P < 0.05$).

expression (**Figure 5**), indicating that the inhibition of miR-21 can lower the content of inflammatory factors at the lesion site, thereby reducing the incidence of inflammatory response.

Size of intracranial aneurysm in different objects observed by EVG staining

To investigate the regulatory mechanism of miR-21 in the formation and rupture of intracranial aneurysm through the JNK signaling pathway-mediated inflammatory response, the size of intracranial aneurysm in mice with miR-21 deficiency and mice with miR-21 over-expression was measured. It was found that the decrease of miR-21 level could impede the formation and rupture of intracranial aneurysm, and the size [(0.3 ± 0.12) cm] and elasticity of intracranial aneurysm in mice with miR-21 deficiency were remarkably smaller than those in mice with miR-21 over-expression [(0.8 ± 0.25) cm] ($P < 0.05$) (**Figure 6**).

Discussion

Intracranial aneurysm is a kind of intracranial disease caused by the abnormal dilation of intracranial arteries [14]. Its clinical manifestations are not obvious and the corresponding symptoms will not be clearly observed until the rupture of intracranial aneurysm, such as subarachnoid hemorrhage. According to clinical statistics [15-17], there are usually no obvious malignant symptoms of intracranial aneurysm, but careful nursing is still needed, bringing a great burden to the families. At present, the pathogenesis of intracranial aneurysm has no definite conclusion, so there have not been any effective treatments. Studies have suggested that the occurrence of intracranial aneurysm may have a certain correlation with vascular inflammation [18-20]. In the present study, the regulatory mechanism of miR-21 in the formation and rupture of intracranial aneurysm through the JNK signaling pathway-mediated inflammatory response was explored for the first time. It was found that compared with healthy mice, mice with intracranial aneurysm had a significantly increased transcription level of miR-21, showing a significant difference ($P < 0.05$). It is reported in related literature that miR-21 can be involved in many metabolic processes through regulating the JNK signaling

pathway in the human body. For example, studies have found that the JNK signaling pathway exists mainly as a pro-apoptotic kinase in the human body, which can participate in such processes as the death receptor pathway, mitochondrial apoptosis pathway, and oxidative stress pathway in vivo, among which the oxidative stress pathway is closely related to the occurrence of inflammatory response *in vivo*. It has been found in studies that oxidative stress can facilitate the occurrence of inflammatory response through promoting the production of inflammatory factors in the body, thereby eliminating viruses and other foreign bodies. In the present study, it was found that the transcription and translation levels of the key genes in the JNK signaling pathway (JNK1 and JNK2) were significantly inhibited in mice with miR-21 deficiency, while they were significantly promoted in mice with miR-21 over-expression. This suggests that miR-21 can regulate the JNK signaling pathway in mice with intracranial aneurysm. The expressions of important inflammatory factors (IL-6 and TNF-α) in healthy mice and intracranial aneurysm mice with miR-21 deficiency and miR-21 over-expression were detected. The results revealed that the expression levels of IL-6 and TNF-α were obviously lower in mice with miR-21 deficiency than those in intracranial aneurysm mice without treatment, displaying significant differences ($P < 0.05$), while they were obviously higher in mice with miR-21 over-expression than those in intracranial aneurysm mice without treatment, also displaying significant differences ($P < 0.05$). The above findings suggest that miR-21 can inhibit the expressions of related inflammatory factors such as IL-6 and TNF-α through suppressing the JNK signaling pathway. The results of EVG staining showed that the vascular thickness and the degree of aneurysm rupture significantly declined in intracranial aneurysm mice with miR-21 deficiency but were significantly increased in intracranial aneurysm mice with miR-21 over-expression. This indicated that miR-21 can accelerate the formation and rupture of intracranial aneurysm through promoting the production of inflammatory factors.

Conclusion

In the present study, we demonstrated that miR-21 induces the production of inflammation-related factors through the JNK signaling pathway. This led to the formation and rupture of intracranial aneurysm, which provides new insights for the mechanism of inflammatory factors in the formation of intracranial aneurysm.

Disclosure of conflict of interest

None.

Address correspondence to: Xianliang Lai, Department of Neurosurgery, The Second Affiliated Hospital of Nanchang University, No. 1, Minde Road, Nanchang 330006, Jiangxi, China. Tel: +86-791-86299726; Fax: +86-791-86299726; E-mail: xianlianglai313@163.com

References

[1] Arjal RK, Zhu T and Zhou Y. The study of fetal-type posterior cerebral circulation on multislice CT angiography and its influence on cerebral ischemic strokes. Clin Imaging 2014; 38: 221-225.

[2] Lv X, Li Y, Yang X, Jiang C and Wu Z. Potential proneness of fetal-type posterior cerebral artery to vascular insufficiency in parent vessel occlusion of distal posterior cerebral artery aneurysms. J Neurosurg 2012; 117: 284-287.

[3] Alexandre AM, Visconti E, Schiarelli C, Frassanito P and Pedicelli A. Bilateral internal carotid artery segmental agenesis: embryology, common collateral pathways, clinical presentation, and clinical importance of a rare condition. World Neurosurg 2016; 95: 620, e9-e15.

[4] Xu J, Xu L, Wu Z, Chen X, Yu J and Zhang J. Fetal-type posterior cerebral artery: the pitfall of parent artery occlusion for ruptured P2 segment and distal aneurysms. J Neurosurg 2015; 123: 906-914.

[5] Gu Z, Eils R and Schlesner M. Complex heat maps reveal patterns and correlations in multidimensional genomic data. Bioinformatics 2016; 32: 2847-2849.

[6] Halaoui R, Rejon C, Chatterjee SJ, Szymborski J, Meterissian S, Muller WJ, Omeroglu A and McCaffrey L. Progressive polarity loss and luminal collapse disrupt tissue organization in carcinoma. Genes Dev 2017; 31: 1573-1587.

[7] Wei J. miR-34s inhibit osteoblast proliferation and differentiation in the mouse by targeting SATB2. J Cell Biol 2012; 197: 509-521.

[8] Wei J. Glucose uptake and run x2 synergize to orchestrate osteoblast differentiation and bone formation. Cell 2015; 161: 1576-1591.

[9] Li S. Connexin 43 and ERK regulate tension-induced signal transduction in human periodontal ligament fibroblasts. J Orthop Res 2015; 33: 1008-1014.

[10] Han MS, Jung DY, Morel C, Lakhani SA, Kim JK, Flavell RA and Davis RJ. JNK expression by macrophages promotes obesity-induced insulin resistance and inflammation. Science 2013; 339: 218-222.

[11] Leung CT and Brugge JS. Outgrowth of single oncogene-expressing cells from suppressive epithelial environments. Nature 2012; 482: 410-413.

[12] Seeliger C. Five freely circulating miRNAs and bone tissue miRNAs are associated with osteoporotic fractures. J Bone Miner Res 2014; 29: 1718-1728.

[13] Hanahan D and Weinberg RA. Hallmarks of cancer: the next generation. Cell 2011; 144: 646-674.

[14] Shen L. Feedback regulations of miR-21 and MAPKs by Pdcd4 and Spry1 are involved in arsenite-induced cell malignant transformation. PLoS One 2013; 8: e57652.

[15] Kim D, Pertea G, Trapnell C, Pimentel H, Kelley R and Salzberg SL. TopHat2: accurate alignment of transcriptomes in the presence of insertions, deletions, and gene fusions. Genome Biology 2013; 14: R36.

[16] Bae Y. miRNA-34c regulates Notch signaling during bone development. Hum Mol Genet 2012; 21: 2991-3000.

[17] Kim KM, Kang HS, Lee WJ, Cho YD, Kim JE and Han MH. Clinical significance of the circle of Willis in intracranial atherosclerotic stenosis. J Neurointerv Surg 2016; 8: 251-255.

[18] Xu J, Yu Y, Wu X, Wu Y, Jiang C, Wang S, Huang Q and Liu J. Morphological and hemodynamic analysis of mirror posterior communicating artery aneurysms. PLoS One 2013; 8: e55413.

[19] Lochner P, Golaszewski S, Caleri F, Ladurner G, Tezzon F, Zuccoli G and Nardone R. Posterior circulation ischemia in patients with fetal-type circle of Willis and hypoplastic vertebrobasilar system. Neurol Sci 2011; 32: 1143-1146.

[20] Lin W, Ma X, Deng D and Li Y. Hemodynamics in the circle of Willis with internal carotid artery stenosis under cervical rotatory manipulation: a finite element analysis. Med Sci Monit 2015; 21: 1820-1826.